

# The Vimos VLT Deep Survey

## Stellar mass segregation and large-scale galaxy environment in the redshift range $0.2 < z < 1.4^*$

M. Scodreggio<sup>1</sup>, D. Vergani<sup>2,1</sup>, O. Cucciati<sup>3,10</sup>, A. Iovino<sup>3</sup>, P. Franzetti<sup>1</sup>, B. Garilli<sup>1</sup>, F. Lamareille<sup>4</sup>, M. Bolzonella<sup>5</sup>, L. Pozzetti<sup>5</sup>, U. Abbas<sup>6,25</sup>, C. Marinoni<sup>11</sup>, T. Contini<sup>4</sup>, D. Bottini<sup>1</sup>, V. Le Brun<sup>6</sup>, O. Le Fèvre<sup>6</sup>, D. Maccagni<sup>1</sup>, R. Scaramella<sup>7,12</sup>, L. Tresse<sup>6</sup>, G. Vettolani<sup>7</sup>, A. Zanichelli<sup>7</sup>, C. Adami<sup>6</sup>, S. Arnouts<sup>13,6</sup>, S. Bardelli<sup>5</sup>, A. Cappi<sup>5</sup>, S. Charlot<sup>8,14</sup>, P. Ciliegi<sup>5</sup>, S. Foucaud<sup>15</sup>, I. Gavignaud<sup>16</sup>, L. Guzzo<sup>3</sup>, O. Ilbert<sup>17</sup>, H. J. McCracken<sup>8,18</sup>, B. Marano<sup>2</sup>, A. Mazure<sup>6</sup>, B. Meneux<sup>19,20</sup>, R. Merighi<sup>5</sup>, S. Paltani<sup>21,22</sup>, R. Pellò<sup>4</sup>, A. Pollo<sup>23,24</sup>, M. Radovich<sup>9</sup>, G. Zamorani<sup>5</sup>, E. Zucca<sup>5</sup>, M. Bondi<sup>7</sup>, A. Bongiorno<sup>19</sup>, J. Brinchmann<sup>26,27</sup>, S. de la Torre<sup>6</sup>, L. de Ravel<sup>6</sup>, L. Gregorini<sup>7</sup>, P. Memeo<sup>1</sup>, E. Perez-Montero<sup>4</sup>, Y. Mellier<sup>8,18</sup>, S. Temporin<sup>28</sup>, and C. J. Walcher<sup>6</sup>

(Affiliations can be found after the references)

Received 3 July 2008 / Accepted 23 February 2009

### ABSTRACT

**Context.** Hierarchical models of galaxy formation predict that the properties of a dark matter halo depend on the large-scale environment surrounding the halo. As a result of this correlation, we expect massive haloes to be present in larger number in overdense regions than in underdense ones. Given that a correlation exists between a galaxy stellar mass and the hosting dark matter halo mass, the segregation in dark matter halo mass should then result in a segregation in the distribution of stellar mass in the galaxy population.

**Aims.** In this work we study the distribution of galaxy stellar mass and rest-frame optical color as a function of the large-scale galaxy distribution using the VLT VIMOS Deep Survey sample, in order to verify the presence of segregation in the properties of the galaxy population.

**Methods.** We use VVDS redshift measurements and multi-band photometric data to derive estimates of the stellar mass, rest-frame optical color, and of the large-scale galaxy density, on a scale of approximately 8 Mpc, for a sample of 5619 galaxies in the redshift range  $0.2 < z < 1.4$ .

**Results.** We observe a significant mass and optical color segregation over the whole redshift interval covered by our sample, such that the median value of the mass distribution is larger and the rest-frame optical color is redder in regions of high galaxy density. The amplitude of the mass segregation changes little with redshift, at least in the high stellar mass regime that we can uniformly sample over the  $0.2 < z < 1.4$  redshift interval. The color segregation, instead, decreases significantly for  $z > 0.7$ . However, when we consider only galaxies in narrow bins of stellar mass, in order to exclude the effects of stellar mass segregation on galaxy properties, we no longer observe any significant color segregation.

**Key words.** galaxies: formation – galaxies: evolution – galaxies: fundamental parameters – cosmology: observations

## 1. Introduction

It is well known that galaxy properties depend on the environment in which the galaxies lie. The two best and longest known examples of such an environmental dependence are the galaxy morphology-density relation (Dressler 1980), that describes the increasing fraction of early-type galaxies in the galaxy population with the increase of the local galaxy density, and the galaxy HI content deficiency (Giovannelli & Haynes 1985) which is observed in cluster late-type galaxies.

More recently, with the advent of large galaxy surveys comprising samples of tens of thousands of objects, it has become possible to study even subtler environmental effects on galaxy properties. Galaxy color and star formation history appear to be the two properties that are most strongly correlated with the galaxy local environment (Blanton et al. 2005; Ball et al. 2008), although an accurate determination of the typical scale-length over which these effects are generated is still missing. Only over

the last few years has some agreement emerged that such a scale-length must be comparable to that of clusters of galaxies, i.e. of the order of 1 to 2 Mpc (Kauffmann et al. 2004, hereafter Ka04; Blanton & Berlind 2007).

On the other hand it is also well known that physical properties of galaxies are mostly inter-related (see Roberts & Haynes 1994, for a review), and that the galaxy total stellar mass plays a significant role in determining these properties (Scodreggio et al. 2002; Kauffmann et al. 2003). The best known example of such a role is certainly the color-magnitude or color-stellar mass relation observed for both early and late-type galaxies, but it is by now equally clear that stellar mass plays an important role in shaping the star formation history of a galaxy (see for example Gavazzi & Scodreggio 1996; Kauffmann et al. 2003; Heavens et al. 2004).

This complex set of inter-relations among environment, galaxy properties, and galaxy stellar mass is certainly part of the reason why the decades old argument about which agent, between “nature” and “nurture”, is the primary driver of galaxy differential evolution, is still far from being settled.

A relatively recent addition to the debate on this subject is a scenario where galaxy properties depend exclusively on the

\* Based on data obtained with the European Southern Observatory Very Large Telescope, Paranal, Chile, program 070.A-9007(A), and on data obtained at the Canada-France-Hawaii Telescope, operated by the CNRS of France, CNRC in Canada and the University of Hawaii.

mass and formation history of the dark matter halo in which the galaxies are formed, but they appear to be correlated with the large scale environment properties purely because of a correlation between halo properties and the large scale environment that surrounds the halo (such a correlation is predicted by hierarchical models, see for example [Mo & White 1996](#); [Sheth & Tormen 2002](#)). This possibility, discussed explicitly by [Abbas & Sheth \(2005, 2006\)](#), is also the basic assumption behind the halo-model descriptions of galaxy clustering that have been used quite successfully in the recent past. In particular, hierarchical models predict the ratio of massive to low mass dark matter halos to be higher in dense environments than it is in under-dense ones ([Mo & White 1996](#)), and simulations show that this is indeed the case ([Sheth & Tormen 2002](#); [Abbas & Sheth 2005](#)), even when the large scale environment is defined using the standard scale length of 8 Mpc (significantly larger than the 1–2 Mpc scale typical of galaxy clusters, which is the scale length over which true environmental effects are expected to be active). Since a good correlation exists between galaxy stellar mass and dark matter halo mass, spanning a large range of stellar masses and galaxy types (e.g. [Mandelbaum et al. 2006](#); [Yang et al. 2007](#)), we can directly translate the dark matter halo mass segregation prediction of hierarchical models into a stellar mass segregation prediction.

Observationally, such a segregation has been demonstrated to exist with reasonable certainty only in the local Universe, using SDSS data, by [Ka04](#). The magnitude of this effect is rather small, with the median stellar mass of galaxies in the densest environments probed by the SDSS data being only twice as large as the one of galaxies in the most under-dense environments (see [Ka04](#) for the details). At higher redshift the effect has never been thoroughly analyzed, except for a brief mentioning of a qualitatively similar result by [Bundy et al. \(2006\)](#), while discussing the stellar mass function for the galaxies in the DEEP2 sample. Similar conclusions have been obtained by [Bolzonella et al.](#) (in preparation), while studying the stellar mass function for the galaxies in the zCOSMOS sample ([Lilly et al. 2007](#)).

In this paper we use the data from the VIMOS-VLT Deep Survey ([Le Fèvre et al. 2005](#)) to extend the [Ka04](#) result, discussing the observational evidence for the presence of a stellar mass segregation over the whole redshift interval from  $z \sim 0.2$  (approximately the upper limit of the SDSS sample) up to  $z \sim 1.4$  (above this redshift our sample becomes too sparse, and our stellar mass estimates quite uncertain), and for a possible evolution in its strength. We also re-analyze the presence of color segregation in this redshift interval (a topic extensively discussed in [Cucciati et al. 2006](#), hereafter [Cu06](#)), and discuss the correlation between mass and color segregation. Section 2 of the paper briefly summarizes the data used in this work, while Sects. 3 and 4 discuss the evidence for stellar mass segregation and the connection between color and stellar mass segregation, respectively.

## 2. The data

In this work we use the observations of the VIMOS-VLT Deep Survey (VVDS, [Le Fèvre et al. 2005](#)) to derive stellar masses and local galaxy densities for a large sample of galaxies over an extended redshift interval.

The VVDS Deep is a purely magnitude limited redshift survey targeting a random subset of an almost complete sample of galaxies in the magnitude range  $17.5 < I_{AB} < 24.0$  (see [McCracken et al. 2003](#) for details on the photometric parent sample) in the VVDS 0226-04 field (hereafter VVDS-F02). Spectroscopic observations with the VIMOS multi-object spectrograph were carried out using 1 arcsec wide slits and the

LRred grism, covering the spectral range from 5500 to 9400 Å, with an effective resolution of  $R \sim 230$  at 7500 Å. All data have been reduced using the VIMOS Interactive Pipeline and Graphical Interface (VIPGI, [Scodeggio et al. 2005](#); [Zanichelli et al. 2005](#)). Highly reliable redshift measurements were obtained for 7528 objects, which corresponds to a sampling rate of approximately 23% of the complete parent photometric sample. In this work we use only galaxies with redshift within the  $0.2 < z < 1.4$  interval, for a total sample of 5884 objects. Within this redshift range the spectral coverage of our sample is basically uniform for galaxies of all spectral types. A comparison between the relative abundance of different spectral types in the spectroscopic and in the parent photometric sample shows that any bias against early-type galaxies in the spectroscopic sample (due to the lack of emission lines, which in turn makes the redshift estimate more difficult to obtain) is limited below the five percent level over the whole redshift range (see the discussion in [Franzetti et al. 2007](#)).

Stellar mass estimates were obtained for all these objects using the GOSSIP spectral energy distribution modeling software ([Franzetti et al. 2008](#)), taking advantage of the multi-band photometric observations available in the VVDS-F02 field, including BVRI data from the CFHT ([McCracken et al. 2003](#)), *U*-band data from the ESO-MPI 2.2 m telescope ([Radovich et al. 2004](#)), *ubvrz* data from the CFHT Legacy Survey ([McCracken et al. 2007](#)), *J* and *Ks*-band data from SOFI at the NTT ([Iovino et al. 2005](#); [Temporin et al. 2008](#)) and from the UKIDSS survey ([Lawrence et al. 2007](#)), 3.6 micron data from the Spitzer-IRAC SWIRE survey ([Lonsdale et al. 2003](#)). The photometric and spectroscopic data were fitted with a grid of stellar population models, generated using the PEGASE2 population synthesis code ([Fioc & Rocca-Volmerange 1997](#)), assuming a set of “delayed” star formation histories (see [Gavazzi et al. 2002](#) for details), and a [Salpeter \(1955\)](#) initial mass function. Further details on the derivation of the stellar masses are presented in [Vergani et al. \(2008\)](#), see also [Pozzetti et al. 2007](#).

Local galaxy densities were obtained computing the three-dimensional number density contrast for galaxies above a certain luminosity threshold in the spectroscopic sample, within a fixed comoving volume. The point-like galaxy distribution was smoothed with a Gaussian filter with a sigma of 5 Mpc, roughly equivalent in volume to a top-hat spherical filter with a sphere radius of 8 Mpc. Further details on the estimation of the local galaxy density are given in [Cu06](#). The choice of this smoothing length has been dictated by the sample properties, mostly by the fact that the mean inter-galaxy separation typical of the VVDS Deep sample is of approximately 4.5 Mpc at the peak of the sample redshift distribution, and even larger at the low and high redshift ends of the distribution. The relatively large value for the smoothing length has also the advantage of mitigating the effects of redshift-space distortions created by galaxy peculiar motions in overdense regions on the density estimates (see [Fig. 2](#) in [Cu06](#)).

To avoid using very uncertain density contrast estimates we have removed from the sample objects that are located at the edges of the volume sampled by the VVDS Deep, for which only one third or less of the comoving volume used to sample the galaxy density contrast is effectively inside the survey volume. Therefore our final sample is composed of 5619 galaxies.

## 3. Stellar mass segregation

If a correlation exists between stellar mass and dark matter halo mass on one side, and the large scale environment properties on

**Table 1.** Sample general properties.

Redshift bin	Median $z$	$\text{Log}(M_{\text{limit}}/M_{\odot})$	$N(> M_{\text{limit}})$
0.2–0.5	0.40	9.0	722
0.5–0.7	0.61	9.5	878
0.7–0.9	0.82	9.8	844
0.9–1.4	1.12	10.3	692

the other side, we can expect the strength of the observed stellar mass segregation to depend on the range of large-scale galaxy densities being considered. Indeed the results presented by Ka04 for the SDSS sample show such a progressive increase in the median stellar mass for samples of galaxies that range from isolated objects to objects in high density environments (see their Fig. 3). The global change in median mass is small, only a factor of 2 when going from the lowermost to the highest density sample, but nonetheless the large statistical sample provided by the SDSS dataset makes this a very robust result.

To extend this result to higher redshift using the VVDS Deep sample, we have to deal with the fact that the magnitude limited nature of the sample produces a stellar mass completeness limit which varies significantly with redshift. As the stellar mass is correlated with galaxy color, and galaxy color is correlated with environment, the only meaningful way we have to search for a possible mass segregation effect in our data is to make sure we are using a mass complete sample at all redshifts. Some discussion about the mass completeness of the VVDS Deep sample has already been presented in Pozzetti et al. (2007), and was further extended in Vergani et al. (2008) and in Meneux et al. (2008, see their Fig. 3) to better take into account the differential mass limit as a function of galaxy color in our sample. Using these results, we have divided our samples into 4 redshift bins, each one with its own stellar mass completeness limit, as listed in Table 1. The table lists the limits adopted for the different redshift bins, the median redshift for the objects in the stellar mass complete sample, the logarithm of the stellar mass completeness limit, in solar mass units, and the number of objects in such a sample. Following the results presented by Meneux et al. (2008) on the stellar mass completeness, and the discussion presented by Franzetti et al. (2007) on the uniformity of the VVDS spectral coverage as a function of spectral type, we can be confident that any color or mass-dependent incompleteness in these 4 samples is limited below the 5 percent level, and it cannot therefore have any significant impact on the results presented below.

Because of the relatively small number of objects within any redshift bin we are considering, we can only partition the sample in a limited number of large-scale environments. In this work we consider a partition of the various environments according to the estimated galaxy number density contrast. For the total VVDS Deep galaxy sample described in Sect. 2 we obtained the distribution of the density contrast values, and for this work, unless stated differently, we consider as galaxies in a low density environment those objects for which the density contrast value is in the lower quartile of the distribution. Conversely, we consider as galaxies in a high density environment those objects for which the density contrast value is in the upper quartile of the distribution. As already discussed in Cu06, the separation between these two extremes of the density distribution is very robust when using a smoothing length of approximately 8 Mpc, which is the value used in this work.

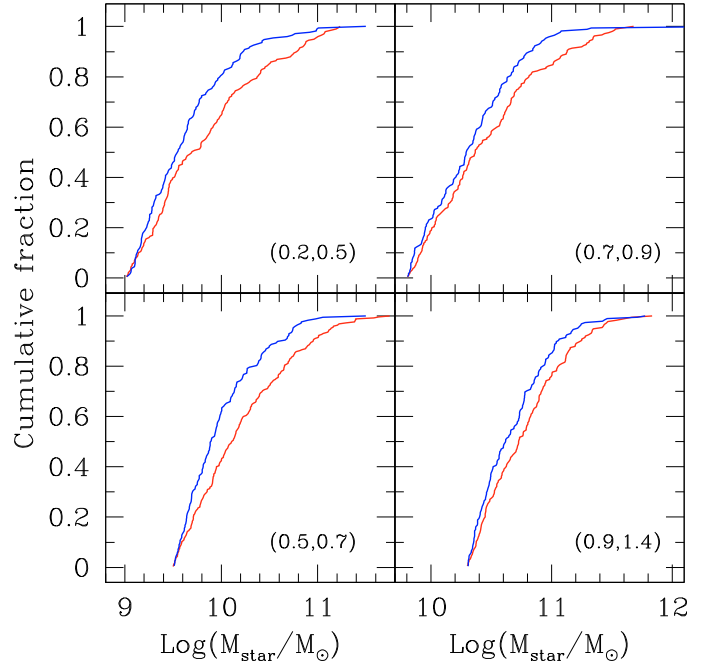


**Fig. 1.** The cumulative mass distribution for the galaxies in the *lower* (blue line) and *upper* (red line) quartile of the overall density distribution in four redshift bins, identified at the *bottom of each plot*; only galaxies above the stellar mass completeness limit appropriate for their redshift interval are considered.

We find that a significant stellar mass segregation is present throughout the VVDS Deep sample used here, up to a redshift of 1.4 (the median  $z$  value for our highest redshift bin being 1.12). Figure 1 shows such a segregation, plotting the integral distribution of stellar mass values for galaxies in the four redshift intervals listed in Table 1, limited to the mass complete samples of objects with  $\text{Log } M_{\text{star}} > \text{Log } M_{\text{limit}}$ ; this is the analogous of Fig. 3 in Ka04. It is quite clear from this plot how the stellar mass distribution in the high density environments is skewed towards higher masses with respect to the distribution in the low density environments. The statistical significance of the observed segregation is at the three-sigma level or above for the three lower redshift bins, while it is only at the two-sigma level for the highest redshift bin, partly because of the lower number of objects we have in that bin.

As expected, given the Ka04 results, we observe that the strength of this segregation depends mildly on how much the low and high density environments are differentiated. In Fig. 2 we show, limited to the redshift bin  $0.5 < z < 0.7$ , the median values for the stellar mass distribution for galaxies in low and high density environments as a function of how extreme we take these two environments to be. Therefore in this case we do not consider just objects in the lowermost or highest quartile (i.e. 25% extremes) of the galaxy density contrast distribution, but also those in the lower and upper half (i.e. 50% extreme) of the distribution, and those in the lower and upper 10% of the distribution (10% extremes). Together with the median values we also plot the associated uncertainties, derived using a bootstrap procedure. Although the separation of the median stellar mass values increases as we move towards the extremes of the density distribution (i.e. towards the extremes of the environment), the statistical significance of these differences remains approximately constant, according to a two-population Kolmogorov-Smirnov test applied to the full stellar mass distribution, because

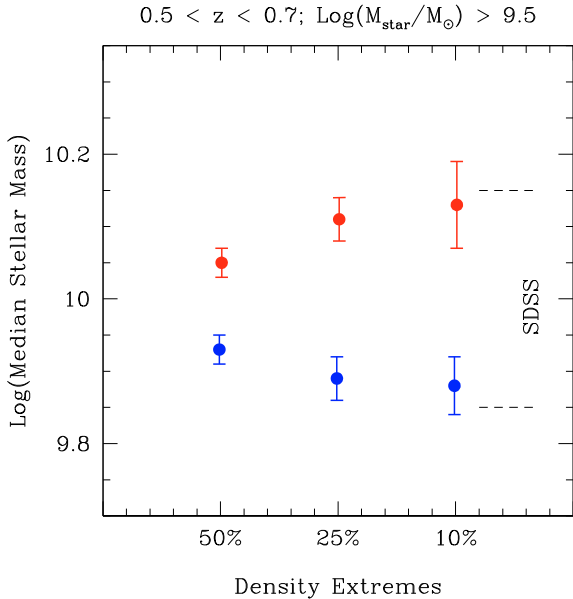


**Fig. 2.** Median values of the mass distribution for galaxies in the lower (blue points) and upper (red points) extreme of the overall density distribution, for three different definitions of extreme: upper and lower half of the distribution, or 50% extreme; upper and lower quartile of the distribution, or 25% extreme; upper and lower 10% of the distribution. Only galaxies in the redshift bin  $0.5 < z < 0.7$  and above the mass completeness limit  $\log(M_{\text{limit}}/M_{\odot}) = 9.5$  are considered in this plot. The error bars represent the bootstrap-based uncertainty estimate in the median value determination. As a reference, the amplitude of the median stellar mass offset measured in the SDSS sample is given by the two dashed lines to the right of the plot (see text for details).

of the decreasing number of objects in the more extreme samples. Therefore the significance with which we measure mass segregation between low and high density environments is always approximately 3 sigmas (i.e. the probability that the two stellar mass distributions are actually drawn from the same parent population is always in the 0.1–0.5 percent range). Similar results are obtained for the other redshift bins we are considering in this work. Purely as a reference, the offset in median stellar mass measured by Ka04 in the two most extreme environments they sampled is indicated in the figure by the two dashed lines on the right of the plot (the mass values where the two lines are drawn are arbitrary), although we must remark that the mass completeness limit for that sample, and the definition of environmental densities are different from those used in this work.

Finally, to examine in detail if and how this mass segregation evolves with cosmic time, we have defined a subsample of 1872 galaxies, limited to objects with  $\log M_{\text{star}}/M_{\odot} > 10.3$ , which is complete in stellar mass over the full redshift range sampled by our data. Figure 3 shows the median stellar mass value for galaxies in low and high density environments, over four redshift bins (those listed in Table 1). As in the previous figure, we also plot the uncertainty in the median estimates. Although we observe a small increase in the strength of the mass segregation (as measured from the median value of the mass distribution), from a redshift of approximately 1.1 down to a redshift of approximately 0.4, this change is not statistically significant: if we compare any two stellar mass distributions for the same environment, but in different redshift bins, we find a probability of more than 50 percent for the two to be drawn from the same parent population (according to a two-population Kolmogorov-Smirnov test). This is true for both the low and the

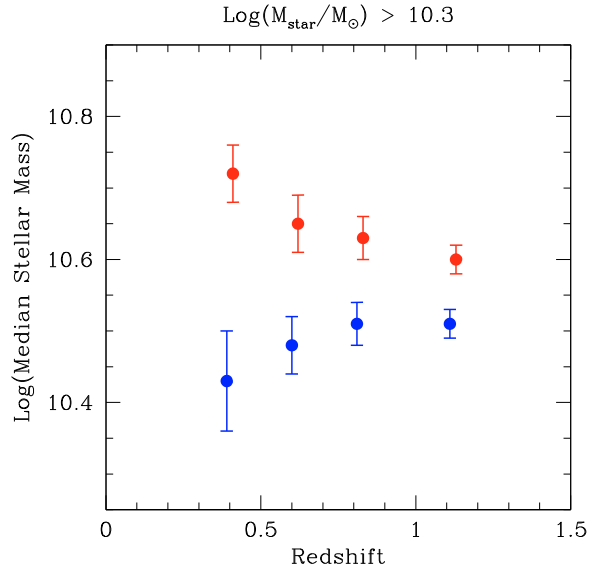


**Fig. 3.** Median values of the mass distribution for galaxies in the lower (blue points) and upper (red points) quartiles of the overall density distribution, in the 4 redshift bins listed in Table 1. Only galaxies above the common mass completeness limit  $\log(M_{\text{limit}}/M_{\odot}) = 10.3$  are considered. The error bars represent the bootstrap-based uncertainty estimate in the median value determination.

high density environment samples. A significantly larger mass-complete sample of galaxies is needed before we can reliably detect any significant evolution in the strength of the stellar mass segregation from the local Universe to  $z = 1$ .

#### 4. Rest-frame color segregation

Physical properties of galaxies (like their color, dust and gas content, and star formation activity) and their morphologies are significantly inter-related, and it is well documented that the galaxy total stellar mass plays an important role in determining these properties (see for example Scodreggio et al. 2002; Kauffmann et al. 2003). It is therefore natural to expect that some segregation in galaxy properties should be observed, purely as a consequence of the stellar mass segregation we have discussed in the previous section.

Rest-frame galaxy colors are well known to show such a segregation in the local Universe (see for example Blanton et al. 2005; Baldry et al. 2006), mirroring the equally well-known morphology-density relation (Dressler 1980). Moving to higher redshift, both the VVDS and the DEEP2 survey have shown that a significant correlation between galaxy color and the large-scale environment exists at least up to  $z \simeq 1$  (see Cu06 and Cooper et al. 2006, respectively), notwithstanding the general trend towards bluer colors which is observed when moving from the local Universe to  $z \simeq 1$ . In particular Cu06, by examining the fraction of red and blue galaxies in different large-scale environments sampled by the VVDS dataset, have shown that, up to  $z < 0.9$ , one observes the locally well known correlation between the fraction of red galaxies and the large-scale density of galaxies. At higher redshift ( $0.9 < z < 1.5$ ) the correlation basically disappears, as more and more massive galaxies become actively star-forming, and it is even possible that the correlation reverses completely, with a predominance of blue galaxies in high-density environments at  $z \simeq 1.5$ .

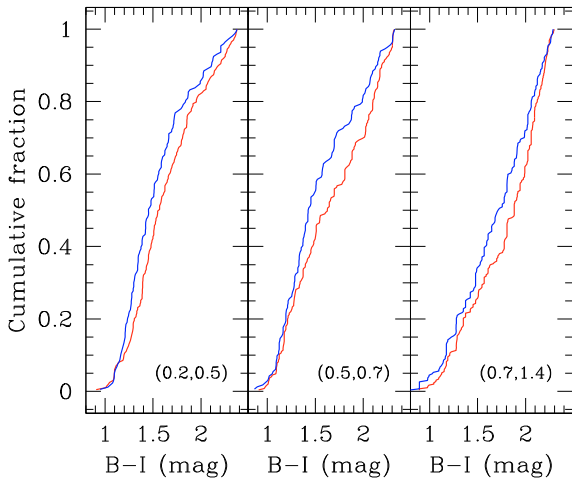


**Fig. 4.** The cumulative rest-frame  $B - I$  color distribution for the galaxies in the *lower* (blue line) and *upper* (red line) quartile of the overall density distribution in the redshift bins  $0.2 < z < 0.5$ ,  $0.5 < z < 0.7$  and  $0.7 < z < 1.4$  respectively.

In Fig. 4 we confirm and extend the Cu06 result by showing the presence of a significant rest-frame color segregation in the VVDS dataset, not only for volume-limited datasets, but also for mass complete ones. Here we plot the integral distributions of rest-frame  $B - I$  color values for galaxies in the first two redshift intervals listed in Table 1 separately, and for galaxies in the last two redshift intervals grouped together. Within each plot, the whole stellar mass complete sample of objects is considered. Here again, because of the completeness in stellar mass and in spectral type coverage already discussed in Sect. 3, we can confidently state that the color distributions for objects in low and high density environments are statistically different at the 3-sigma level (having a probability of being drawn from the same parent population of 0.2–0.4 percent, as estimated from a two-population Kolmogorov-Smirnov test) for  $z < 0.7$ , while in the redshift interval  $0.7 < z < 1.4$  the significance drops to approximately the 2-sigma level. This result is in agreement with the earlier findings of Cu06 about the disappearance of the correlation between the fraction of red galaxies and the large-scale density of galaxies for  $z > 0.9$ .

In Fig. 5, on the contrary, we show that the rest-frame color segregation is significantly weaker when we consider only galaxies within relatively small stellar mass bins, to the point that we do not observe any statistically significant difference in the color distribution for galaxies in the low and high density environment. This lack of any residual color segregation is in contrast with some findings from the SDSS sample discussed in Ka04 and in Baldry et al. (2006), that report a significant environmental dependence of galaxy properties, even when considering only objects within relatively small stellar mass bins. One possible explanation for this discrepancy is the very different scale-length over which the local galaxy density is estimated in this work (8 Mpc) and in the SDSS ones (1 Mpc). Another important difference coming into play is the smaller size of the VVDS Deep sample used here, with respect to the SDSS one. It is therefore possible that some segregation in galaxy rest-frame color could still be present in our sample, even when considering narrow mass bins, but the relatively minor strength of this segregation, coupled with the small sample size, could prevent us from

measuring this effect with any statistical significance. This topic will be analyzed in further detail using the larger zCOSMOS sample in a forthcoming paper (Cucciati et al., in preparation).

This discrepancy aside, the observed significant weakening of the galaxy color segregation which is observed when we consider galaxies in relatively narrow stellar mass bins strongly suggests that the segregation we observe on 8 Mpc scales is mostly (if not entirely) driven by the underlying stellar mass segregation, coupled with the well known color-stellar mass correlation. A similar conclusion could be derived from the observed absence of any environmental effects on the locus of the color-stellar mass relation, both for objects in the red sequence and in the blue cloud, which was discussed by Cassata et al. (2007), using the data from the COSMOS survey (Scoville et al. 2007).

## 5. Conclusions

A significant stellar mass segregation as a function of the large-scale galaxy environment, the latter defined from the measured galaxy number density contrast within scales of approximately 8 Mpc, is observed in the VVDS sample over the whole redshift range from  $z = 0.2$  up to  $z \sim 1.4$ : the stellar mass distribution of high density regions shows the presence of a larger number of high stellar mass galaxies than the distribution observed in low density regions. The scales over which this segregation is observed are much larger than the typical group or cluster scale (approximately 1 Mpc) where environmental effects are expected to play a significant role in shaping galaxy evolution. It is however impossible for us, with the present sample, to evaluate the possibility that the mass segregation signature we observe on the 8 Mpc scale could just be a diluted signal produced by a much stronger segregation at the 1 Mpc scale, because the typical mean interparticle separation of the VVDS Deep sample does not allow us to reliably derive galaxy densities on the 1 Mpc scale. It is remarkable however that the observed segregation is in rather good agreement with the expectations from the hierarchical models, which predict a very similar segregation of dark matter haloes (the strength in the mass segregation of the dark matter haloes is expected to be 2–3 times stronger than the observed stellar mass one, but part of this discrepancy could be explained by the presence of a large number of very low mass haloes in the underdense regions that do not host any galaxies, see Abbas & Sheth 2005). The strength of the observed stellar mass segregation decreases marginally with increasing redshift, from  $z = 0.4$  to  $z = 1.2$ , but within the relatively small statistics offered by the mass-complete VVDS galaxy sample, such a weakening of the mass segregation cannot be considered as a statistically robust result.

A significant rest-frame galaxy color segregation is observed as well, mirroring the stellar mass one. However we have demonstrated that a large fraction of this color segregation is simply a reflection of the stellar mass segregation, via the well known correlation between stellar mass and galaxy color. In fact, when we compare rest-frame colors for galaxies with stellar mass within a narrow range, we do not find significant differences in the color distribution as a function of the large-scale environment.

These results, coupled with the observed differential galaxy clustering reported in Abbas & Sheth (2006), provide strong support for the hypothesis that a large fraction of the observed environmental effects on galaxy properties, like broadband optical color, or star formation history, are just the reflection of the correlation between galaxy stellar mass and the galaxy hosting dark matter halo mass, which in turn correlates with the surrounding large scale environment. Further discussion on the correlation

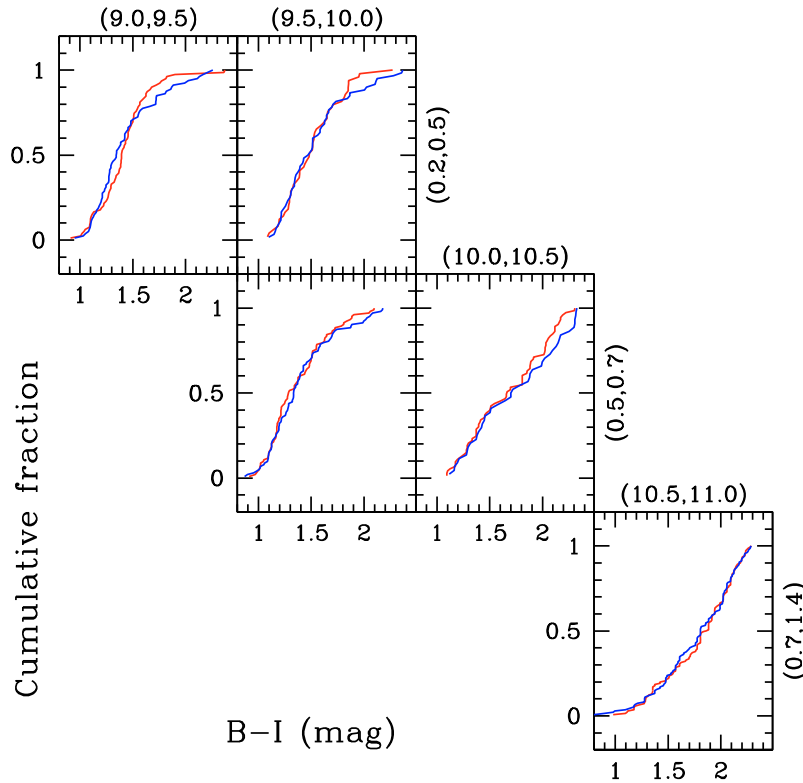


**Fig. 5.** The cumulative rest-frame  $B - I$  color distribution for the galaxies in the lower (blue line) and upper (red line) quartile of the overall density distribution in the same redshift bins used in the previous figure (as indicated to the right of the panels), but considering only galaxies in small stellar mass bins (indicated at the top of the various panels).

between star formation activity and the large-scale environment where galaxies are located will be presented in a forthcoming paper (Vergani et al., in preparation).

*Acknowledgements.* M.S. would like to thank Frank van den Bosch for a very useful discussion on environmental effects, that provided the motivation for this work.

This research has been developed within the framework of the VVDS consortium. This work has been partially supported by the CNRS-INSU and its Programme National de Cosmologie (France), and by Italian Ministry (MIUR) grants COFIN2000 (MM02037133) and COFIN2003 (No. 2003020150) and by INAF grants (PRIN-INAF 2005). D.V. acknowledges the support through a Marie Curie ERG, funded by the European Commission under contract No. MERG-CT-2005-021704.

The VLT-VIMOS observations have been carried out on guaranteed time (GTO) allocated by the European Southern Observatory (ESO) to the VIRMOS consortium, under a contractual agreement between the Centre National de la Recherche Scientifique of France, heading a consortium of French and Italian institutes, and ESO, to design, manufacture and test the VIMOS instrument. Based on observations obtained with MegaPrime/MegaCam, a joint project of CFHT and CEA/DAPNIA, at the Canada-France-Hawaii Telescope (CFHT) which is operated by the National Research Council (NRC) of Canada, the Institut National des Science de l'Univers of the Centre National de la Recherche Scientifique (CNRS) of France, and the University of Hawaii. This work is based in part on data products produced at TERAPIX and the Canadian Astronomy Data Centre as part of the Canada-France-Hawaii Telescope Legacy Survey, a collaborative project of NRC and CNRS.

## References

- Abbas, U., & Sheth, R. K. 2005, *MNRAS*, 364, 1327  
 Abbas, U., & Sheth, R. K. 2006, *MNRAS*, 372, 1749  
 Baldry, I. K., Balogh, M. L., Bower, R. G., et al. 2006, *MNRAS*, 373, 469  
 Ball, N. M., Loveday, J., & Brunner, R. J. 2008, *MNRAS*, 383, 907  
 Blanton, M. R., & Berlind, A. A. 2007, *ApJ*, 664, 791  
 Blanton, M. R., Eisenstein, D., Hogg, D. W., Schlegel, D. J., & Brinkmann, J. 2005, *ApJ*, 629, 143  
 Bundy, K., Ellis, R. S., Conselice, C. J., et al. 2006, *ApJ*, 651, 120  
 Cassata, P., Guzzo, L., Franceschini, A., et al. 2007, *ApJS*, 172, 270  
 Cooper, M. C., Newman, J. A., Croton, D. J., et al. 2006, *MNRAS*, 370, 198  
 Cucciati, O., Iovino, A., Marinoni, C., et al. 2006, *A&A*, 458, 39  
 Dressler, A. 1980, *ApJ*, 236, 351  
 Fioc, M., & Rocca-Volmerange, B. 1997, *A&A*, 326, 950  
 Franzetti, P., Scodeggio, M., Garilli, B., et al. 2007, *A&A*, 465, 711  
 Franzetti, P., Scodeggio, M., Garilli, B., Fumana, M., & Paioro, L. 2008, in *Astronomical Data Analysis Software and Systems XVII*, ed. R. W. Argyle, P. S. Bunclark, & J. R. Lewis, ASP Conf. Ser., 394, 642  
 Gavazzi, G., & Scodeggio, M. 1996, *A&A*, 312, L29  
 Gavazzi, G., Bonfanti, C., Sanvito, G., Boselli, A., & Scodeggio, M. 2002, *ApJ*, 576, 135  
 Giovanelli, R., & Haynes, M. P. 1985, *ApJ*, 292, 404  
 Heavens, A., Panter, B., Jimenez, R., & Dunlop, J. 2004, *Nature*, 428, 625  
 Iovino, A., McCracken, H. J., Garilli, B., et al. 2005, *A&A*, 442, 423  
 Kauffmann, G., Heckman, T. M., White, S. D. M., et al. 2003, *MNRAS*, 341, 54  
 Kauffmann, G., White, S. D. M., Heckman, T. M., et al. 2004, *MNRAS*, 353, 713  
 Lawrence, A., Warren, S. J., Almaini, O., et al. 2007, *MNRAS*, 379, 1599  
 Le Fèvre, O., Vettolani, G., Garilli, B., et al. 2005, *A&A*, 439, 845  
 Lilly, S. J., Le Fèvre, O., Renzini, A., et al. 2007, *ApJS*, 172, 70  
 Lonsdale, C. J., Smith, H. E., Rowan-Robinson, M., et al. 2003, *PASP*, 115, 897  
 Mandelbaum, R., Seljak, U., Kauffmann, G., Hirata, C. M., & Brinkmann, J. 2006, *MNRAS*, 368, 715  
 McCracken, H. J., Radovich, M., Bertin, E., et al. 2003, *A&A*, 410, 17  
 Meneux, B., Guzzo, L., Garilli, B., et al. 2008, *A&A*, 478, 299  
 Mo, H. J., & White, S. D. M. 1996, *MNRAS*, 282, 347  
 Pozzetti, L., Bolzonella, M., Lamareille, F., et al. 2007, *A&A*, 474, 443  
 Radovich, M., Arnaboldi, M., Ripepi, V., et al. 2004, *A&A*, 417, 51  
 Roberts, M. S., & Haynes, M. P. 1994, *ARA&A*, 32, 115  
 Salpeter, E. E. 1955, *ApJ*, 121, 161  
 Scodeggio, M., Gavazzi, G., Franzetti, P., et al. 2002, *A&A*, 410, 17  
 Scodeggio, M., Franzetti, P., Garilli, B., et al. 2005, *PASP*, 117, 1284  
 Scoville, N., Aussel, H., Brusa, M., et al. 2007, *ApJS*, 172, 1  
 Sheth, R. K., & Tormen, G. 2002, *MNRAS*, 329, 61  
 Tempurin, S., Iovino, A., Bolzonella, M., et al. 2008, *A&A*, 482, 81  
 Vergani, D., Scodeggio, M., Pozzetti, L., et al. 2008, *A&A*, 487, 89

Yang, X., Mo, H. J., van den Bosch, F. C., et al. 2007, *ApJ*, 671, 153  
Zanichelli, A., Garilli, B., Scodreggio, M., et al. 2005, *PASP*, 117, 1271

---

<sup>1</sup> INAF IASF – Milano, via Bassini 15, 20133 Milano, Italy  
e-mail: marcos@lambrate.inaf.it

<sup>2</sup> Università di Bologna, Dipartimento di Astronomia, via Ranzani 1, 40127 Bologna, Italy

<sup>3</sup> INAF – Osservatorio Astronomico di Brera, via Brera 28, 20021 Milan, Italy

<sup>4</sup> Laboratoire d’Astrophysique de Toulouse-Tarbes, Université de Toulouse, CNRS, 14 Av. E. Belin, 31400 France,

<sup>5</sup> INAF – Osservatorio Astronomico di Bologna, via Ranzani 1, 40127 Bologna, Italy

<sup>6</sup> Laboratoire d’Astrophysique de Marseille, UMR 6110 CNRS-Université de Provence, BP 8, 13376 Marseille Cedex 12, France

<sup>7</sup> IRA – INAF, via Gobetti 101, 40129 Bologna, Italy

<sup>8</sup> Institut d’Astrophysique de Paris, UMR 7095, 98 bis Bvd Arago, 75014 Paris, France

<sup>9</sup> INAF – Osservatorio Astronomico di Capodimonte, via Moiariello 16, 80131 Napoli, Italy

<sup>10</sup> Università di Milano-Bicocca, Dipartimento di Fisica, Piazza delle Scienze 3, 20126 Milano, Italy

<sup>11</sup> Centre de Physique Théorique, UMR 6207 CNRS-Université de Provence, 13288 Marseille, France

<sup>12</sup> INAF – Osservatorio Astronomico di Roma, via di Frascati 33, 00040, Monte Porzio Catone, Italy

<sup>13</sup> Canada France Hawaii Telescope corporation, Mamalahoa Hwy, Kamuela, HI-96743, USA

<sup>14</sup> Max Planck Institut für Astrophysik, 85741 Garching, Germany

<sup>15</sup> School of Physics & Astronomy, University of Nottingham, University Park, Nottingham, NG72RD, UK

<sup>16</sup> Astrophysical Institute Potsdam, An der Sternwarte 16, 14482 Potsdam, Germany

<sup>17</sup> Institute for Astronomy, 2680 Woodlawn Dr., University of Hawaii, Honolulu, Hawaii 96822, USA

<sup>18</sup> Observatoire de Paris, LERMA, 61 Av. de l’Observatoire, 75014 Paris, France

<sup>19</sup> Max Planck Institut für Extraterrestrische Physik (MPE), Giessenbachstrasse 1, 85748 Garching bei München, Germany

<sup>20</sup> Universitätssternwarte München, Scheinerstrasse 1, 81679 München, Germany

<sup>21</sup> Integral Science Data Centre, ch. d’Écogia 16, 1290 Versoix, Switzerland

<sup>22</sup> Geneva Observatory, ch. des Maillettes 51, 1290 Sauverny, Switzerland

<sup>23</sup> The Andrzej Soltan Institute for Nuclear Research, ul. Hoza 69, 00-681 Warszawa, Poland

<sup>24</sup> Astronomical Observatory of the Jagiellonian University, ul. Orla 171, 30-244 Kraków, Poland

<sup>25</sup> INAF – Osservatorio Astronomico di Torino, 10025 Pino Torinese, Italy

<sup>26</sup> Centro de Astrofísica da Universidade do Porto, Rua das Estrelas, 4150-762 Porto, Portugal

<sup>27</sup> Leiden Observatory, Leiden University, Postbus 9513, 2300 RA, Leiden, The Netherlands

<sup>28</sup> Institute of Astro- and Particle Physics, Leopold-Franzens-University Innsbruck, Technikerstraße 25, 6020 Innsbruck, Austria